Journal of Applied Research and Technology

www.jart.ccadet.unam.mx
Journal of Applied Research and Technology 17 (2019) 78-91

Original

Amine modified kaolinite clay from Nigeria: A resource for removing Cd^{2+} and Pb^{2+} ions from aqueous solution

Adewale Adewuyi [a, b, *], Fabiano Vargas Pereira [b], Omotayo Anuoluwapo Adewuyi [c]

[a] *Department of Chemical Sciences, Faculty of Natural Sciences, Redeemer's University, Mowe, Ogun state, Nigeria*

[b] *Department of Chemistry, Federal University of Minas Gerais, Av. Antônio Carlos, 6627, Pampulha, CEP 31270-901 Belo Horizonte, MG, Brazil*

[c] *Enviro Africa Limited, plot 182b Kofo Abayomi Street, Victoria Island, Lagos, Nigeria*

Abstract: Kaolinite clay (KC) obtained from redemption camp; Nigeria was modified by surface grafting and investigated for the removal of Pb^{2+} and Cd^{2+} ions from aqueous solution by adsorption. KC and the modified kaolinite clay (MKC) were characterized using X-ray Diffraction analysis (XRD), Scanning Electron Microscopy (SEM), Brunauer-Emmett-Teller (BET) surface area analyzer, Fourier Transform Infrared spectrometer (FTIR), Particle Size Distribution (PSD), zeta potential, elemental analysis (CHNS/O analyzer) and Energy Dispersive Spectroscopy (EDS). Equilibrium, thermodynamics and kinetic studies were conducted by considering the effects of pH, initial metal ion concentration, contact time, adsorbent weight and temperature. Modification of KC increased its equilibrium adsorption capacity from 8.01 mg/g to 24.41 mg/g for Cd^{2+} and from 24.75 mg/g to 36.41 mg/g for Pb^{2+} ions. The adsorption process obeys Freundlich and Temkin isotherms. The adsorption was second-order-kinetic and controlled by both intra-particle and liquid film diffusion. Values of ΔG^{o}, ΔH^{o} and ΔS^{o} for KC and MKC showed a stable adsorbent-adsorbate configuration.

Keywords: Adsorption, Kaolinite clay, Heavy metal, Surface grafting, Wastewater treatment

1. INTRODUCTION

Developing nation such as Nigeria often suffer from discharge of heavy metal ions into fresh water, soil and marine environment causing serious pollution problems. Example of this is the Zamfara (a state in Nigeria) lead poisoning, which is the worst heavy metal incidence in the Nigerian records that claimed the lives of over 500 children within seven months in 2010 (Galadima Garba, Leke, Almustapha, & Adam 2011; Galadima & Garba, 2012). Several efforts have been made in time past to treat polluted or waste water but most of these efforts have

* Corresponding author.
E-mail address: walexy62@yahoo.com (Adewale Adewuyi).
Peer Review under the responsibility of Universidad Nacional Autónoma de México.

suffered from different drawbacks (Adewuyi & Pereira, 2016; Basra, Iqbal, Ur-Rehman, & Ejaz, 2014), mainly cost ineffectiveness and inability to setup and maintain such efforts in poor developing countries of which Nigeria is inclusive.

The choice of method for wastewater treatment is important (Mirbolooki, Amirnezhad, & Pendashteh, 2017) which may have to depend on the concentration, type, and nature of the pollutants present in the wastewater. Among all the methods that have been reported in the past, adsorption still remains less expensive; it can be easily setup and maintained and capable of averting large amount of sludge usually formed during waste water treatment (Bhattacharyya & Gupta, 2006). These properties have made adsorption more promising and attractive in developing nations which are much more affected by water pollution. The type of adsorbent used during adsorption process plays a key role in making the process a success (Pouya, Abolghasemi, Fatoorehchi, Rasem, & Hashemi, 2016). Such adsorbent is expected to be efficient, highly selective, non-toxic, regenerative, readily available and easily recovered from the treated water system. Clay such as kaolinite is a potential material that can function in this regard as an adsorbent for treating waste water (Fan et al., 2009; Nishikiori et al., 2009). Most neat clay have been reported not to be as efficient as activated carbon and zeolite due to their low surface area, low regeneration tendency and poor particle recovery after being spent (Borisover, Gerstl, Burshtein, Yariv, & Mingelgrin, 2008; Laouchedi, Bezzazi, & Aribi, 2017; Unuabonah & Taubert, 2014). However, when modified, the neat clay has the potential of being more efficient than activated carbon and zeolite.

Kaolinite clay is an abundant resource in Nigeria which has received little attention as an adsorbent because of its low cation exchange capacity (3-15 meq/100 g) and its small surface area which is ≤ 20.0 m^2/g (Bhattacharyya & Gupta, 2008; Guerra, Airoldi, & de Sousa, 2008; Manohar, Noeline, & Anirudhan, 2006). There has been report that these challenges may be improved via modification such as activation, intercalation and or chemical surface grafting (Frost, Van Der Gaast, Zbik, Kloprogge, & Paroz, 2002; Kho & Dixon, 200: Sidheswara, Bhat, & Ganguli, 1990). Preferably, modification of kaolinite clay can be achieved by either intercalation or surface grafting (Guerra et al., 2008). Although there has been a number of studies on kaolinite clay for the removal of heavy metals (Bhattacharyya & Gupta, 2008; Gupta & Bhattacharyya, 2008), there is still need to improve on its adsorption capacity via simple and green methods.

The present study investigated the surface modification of KC as a low-cost adsorbent for the treatment of aqueous solution containing Pb^{2+} and Cd^{2+} ions. The effects of adsorbent weight, change in temperature, pH, initial concentration of Pb^{2+} and Cd^{2+} ions and contact time on the removal of Pb^{2+} and Cd^{2+} ions from the aqueous solution by KC and MKC were investigated as well as the mechanism of uptake of these heavy metal ions.

2. MATERIALS AND METHODS

2.1 MATERIALS

KC used was collected from the Redemption Camp at Mowe, Ogun state, Nigeria. After collection, particulate matters such as stones and other metal particles were separated from KC which was further purified using method described by Moore and Reynolds. All chemicals used in this study were purchased from Sigma-Aldrich (Brazil). Experimental solutions containing heavy metal ions were prepared by dissolving appropriate amount of nitrates ($Cd(NO_3)_2$ and $Pb(NO_3)_2$) in deionized water to desired concentrations.

2.2 MODIFICATION OF KC

Mixture of chloroacetic acid (0.06 mole), thionylchloride (0.08 mole) and chloroform (50 mL) was heated to 75°C for 30 min to form chloroacetylchloride (Scheme 1). A 20 g of KC was added to the chloroacetylchloride (after the removal of excess thionylchloride under reduced pressure) which was allowed to react for 6 h under constant stirring at 90°C and finally cooled in ice. Ethylenediamine (100 mL) was added to the solid mass left and stirred for 12 h at 100°C under reflux. The unreacted ethylenediamine was gently removed; cold deionized water was added to the product left and centrifuged thrice for 10 min at 8,500 rpm to remove excess ethylenediamine. The MKC obtained was oven dried at 60°C for 48 h (Scheme 2) with about 98% yield.

2.3 CHARACTERIZATION

The functional groups in KC and MKC were determined using FTIR (Perkin Elmer, spectrum RXI

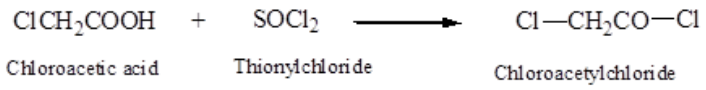

Scheme 1. Synthesis of chloroacetylchloride.

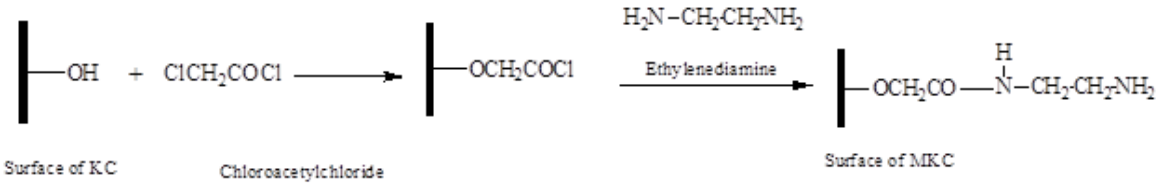

Scheme 2. Preparation of MKC.

83303). KC and MKC were blended with KBr, pressed into pellets and analyzed in the range of 400 - 4500 cm^{-1}. Elemental analysis was achieved using Perkin Elmer series II CHNS/O analyzer (Perkin Elmer, 2400, USA) while information of the surface morphology was obtained using SEM-EDS (FEI quanta 200 3D, dual beam FEG, model EDAX EDS brand, Bruker) with powdered samples being coated with gold using the sputtering technique in order to increase electrical conductivity and the quality of the micrographs. The surface area of KC and MKC was determined by nitrogen adsorption using the BET method in a Quantachrome Autosorb IQ_2 instrument. X-ray diffractometer (XRD-7000X-Ray diffractometer, Shimadzu) with filtered Cu Kα radiation operated at 40 kV and 40 mA was used to obtain the X-ray diffraction pattern. The XRD pattern was recorded from 10 to 80° (2θ), with a scanning speed of 2.00°/min. Particle size distribution and zeta potential were recorded using a zeta potential analyzer (DT1200, Dispersion technology) at 25°C while observing general calculation model for irregular particles. Several measurements were taken using Dispersion technology-AcoustoPhor Zeta size 1201 software (version 5.6.16).

2.4 EQUILIBRIUM STUDY

Batch adsorption equilibrium study was carried out by contacting 0.5 g of KC and MKC separately with 250 mL varying concentration of Cd^{2+} and Pb^{2+} (10 – 100 mg/L) solutions in different 500 mL beaker at 298 K and 200 rpm for 3 h. Several agitations at 298 K and 200 rpm were repeated in order to establish the equilibrium time. Equilibrium concentration of Cd and Pb were determined by withdrawing clear samples at different interval and analyzing using Atomic Absorption Spectrometer (Varian AA240FS).

2.5 EFFECT OF KC AND MKC WEIGHT ON ADSORPTION OF Cd^{2+} AND Pb^{2+} IONS

Effect of KC and MKC weight was evaluated by varying the weight of KC and MKC from 0.1-1.0 g in 250 mL of 100 mg/L solution for 3 h. Concentrations of Cd^{2+} and Pb^{2+} were established after several equilibrium studies. Clear supernatant were withdrawn at different time interval and analyzed using Atomic Absorption Spectrometer (Varian AA240FS).

2.6 EFFECT OF PH ON ADSORPTION OF Cd^{2+} AND Pb^{2+} IONS BY KC AND MKC

A 0.5 g of KC and MKC was separately agitated with 100 mg/L solution of Cd^{2+} and Pb^{2+} ions. This was adjusted over a pH range of 1.70 – 6.60 using 0.1 M HCl and 0.1 M NaOH and stirred at 200 rpm in a 500 mL beaker for 3 h. Clear samples were withdrawn at different intervals and analyzed using Atomic Absorption Spectrometer (Varian AA240FS).

2.7 THERMODYNAMIC STUDY

Thermodynamics of the adsorption of Cd^{2+} and Pb^{2+} on KC and MKC was carried out at different initial concentrations (10 to 100 mg/L) and temperatures ranging from 298 to 333 K. The solutions were stirred at 200 rpm in a 500 mL beaker for 3 h. Clear samples were withdrawn at different intervals and analyzed using Atomic Absorption Spectrometer (Varian AA240FS).

3. RESULT AND DISCUSSION

3.1 CHARACTERIZATION

The XRD results in Fig. 1 reveals prominent peaks at 7.19 Å, 4.11 Å, 3.58 Å, 3.35 Å, 2.98 Å, 2.29Å, 1.82 Å, and

1.49 Å which correspond to kaolinite, quartz, tridymite, kaolinite, quartz, quartz + alunite, quart and kaolinite. Both spectra of KC and MKC looks similar suggesting that the d-spacing of the crystal lattice of KC was not significantly altered as similar peaks were found in both KC and MKC. This observation suggests the modification to be a surface phenomenon.

Structure of kaolinite minerals is expected to have a sheet of corner-sharing tetrahedral linked with a plane of oxygen and hydroxyl groups which are referred to as inner hydroxyls (Saikia & Parthasarathy, 2010). The OH stretching for kaolinite were seen in both KC and MKC at 3697, 3620 and 3452 cm^{-1} as reported by Farmer (1974); this is presented in Fig. 2. Band at around 3620 cm^{-1} was attributed to the inner hydroxyls while band at 3697 cm^{-1} was considered to be vibrational frequencies of the external hydroxyls. The band observed at 3452 cm^{-1} in KC was taken to be the OH vibrational mode for natural hydrous silicates (Saikia & Parthasarathy, 2010). This peak at 3452 cm^{-1} in KC became broader in MKC which appeared at 3439 cm^{-1} suggesting an overlap of the hydroxyl peak with the amine peak formed in MKC. The peaks at 1033 cm^{-1} in KC and MKC may be due to the interference from alunite and or quartz while peak at 914 cm^{-1} could be due to Al-OH vibrational bending. The doublet at 792-777 cm^{-1} in KC and MKC may be due to Si-O-Si inter tetrahedral bridging bonds (McMillan, Wolf, & Poe, 1992). The Al-O-Si and Si-O-Si deformations were seen at 536 and 466 cm^{-1}; respectively while the Si-O frequency was seen at 694 cm^{-1} in both KC and MKC. The CHN analysis results showed the hydrogen content to increase from 2.90 % in KC to 3.96% in MKC. Carbon and nitrogen were found to be 8.88 and 1.20 %; respectively in MKC. The increase in hydrogen content and the presence of carbon and nitrogen in MKC suggests that modification had taken place.

The surface morphology and EDS results of KC and MKC are presented in Fig. 3 and Fig. 4; respectively. The surface morphology of KC is different from that of MKC according to the SEM images in Fig. 3. The flaky-like crystal and fluffy appearance of KC was seen in the micrograph while MKC appears to be fluffier with a more consistent texture than KC. The EDX results for KC and MKC are presented in Fig. 4 which reveals their composition. The BET surface area reveals the surface area of KC to be 16 m^2/g while that of MKC was found to be 13 m^2/g. The particle size distribution is shown in Fig. 5; this was found to be bimodal for KC and monomodal for MKC. The zeta potential for KC and MKC are presented in Fig. 6. As previously reported (Adewuyi & Pereira, 2017), values obtained for zeta potential helped in quantifying the charges at the surfaces of KC and MKC which suggested the degree of stability of KC and MKC and their electrostatic repulsion with other charged particles (Hanaor, Michelazzi, Leonelli, & Sorrell, 2012). In this study, the zeta potential reduced as pH values increased below the pH of 6. In the case of KC, the zeta potential increased as pH increased above 6 but later dropped at pH above 9. In MKC, the zeta potential only slightly increased above pH 6 but dropped immediately. As pH further increased, the zeta potential of MKC kept reducing until pH of 12 when the zeta potential began to increase again. This observation may be due to the presence of the amine groups at the surface of MKC. The distribution of the zeta potential at various pH along the surfaces of KC and MKC has revealed that both KC and MKC are stable in liquid medium, mainly where solid-liquid interaction exists. Moreover, materials with high zeta potential (negative or positive) are known to be better electrically stabilized than materials with low zeta potentials which tend to coagulate or flocculate (Hanaor et al., 2012).

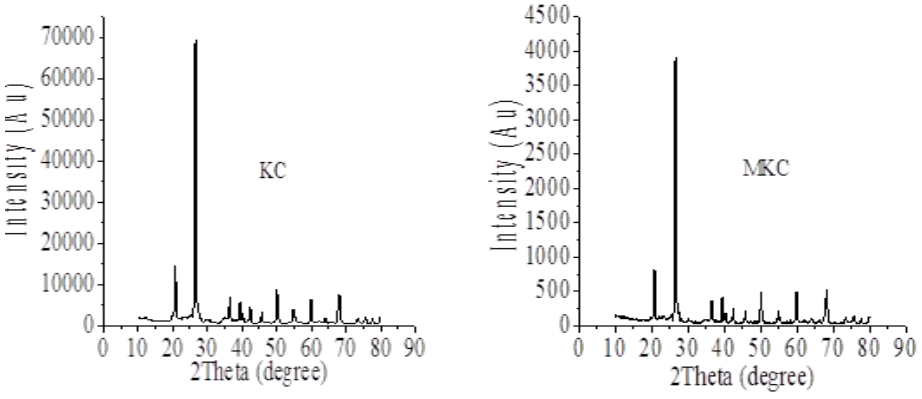

Fig. 1. XRD of KC and MKC.

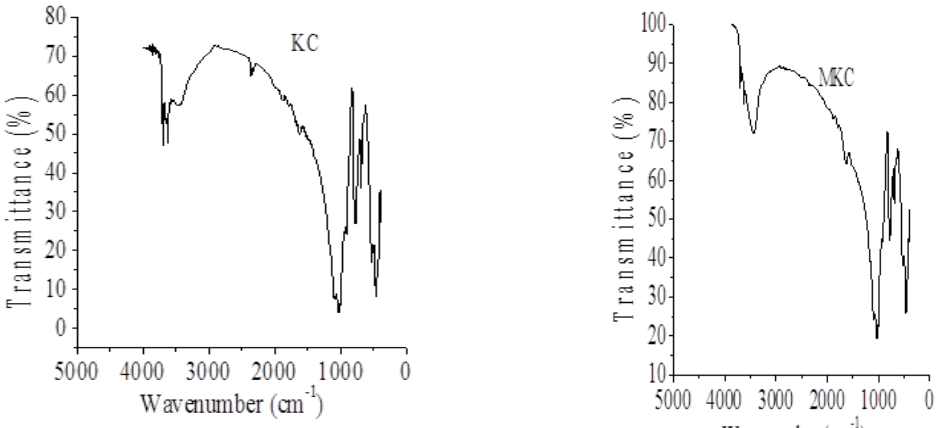

Fig. 2. FTIR results of KC and MKC.

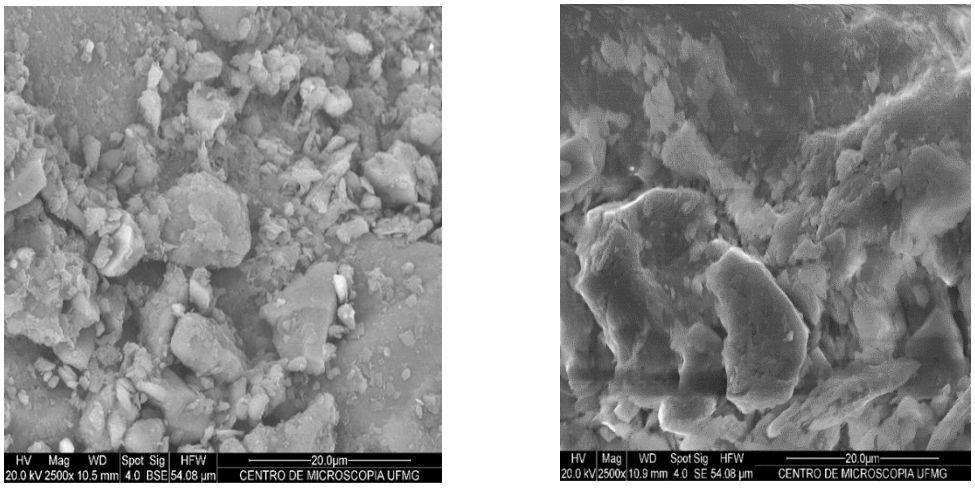

KC MKC

Fig. 3. SEM of KC and MKC

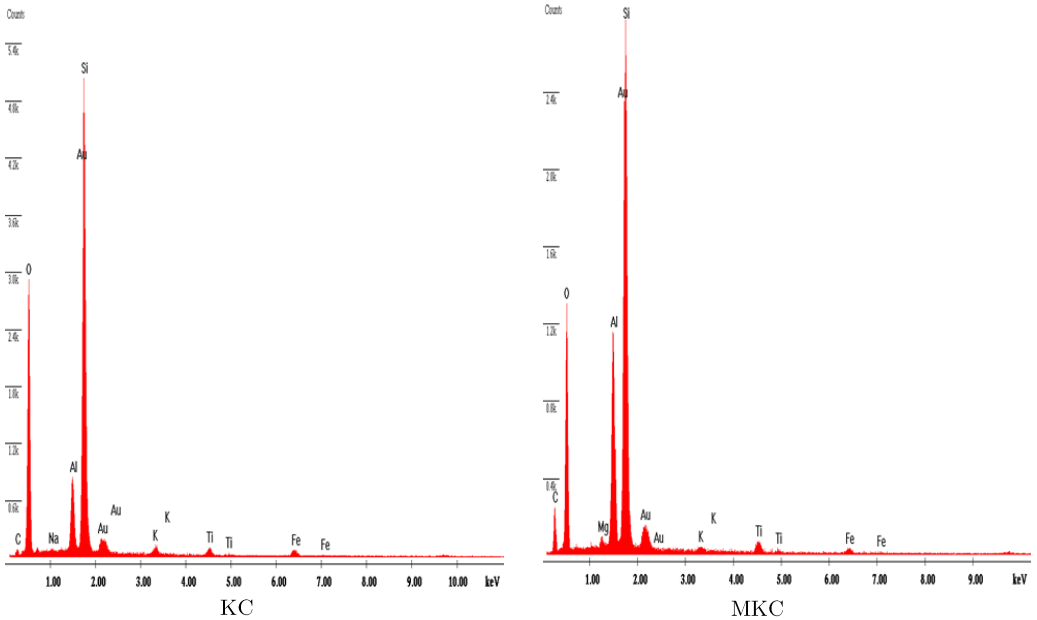

KC MKC

Fig. 4. EDX of KC and MKC.

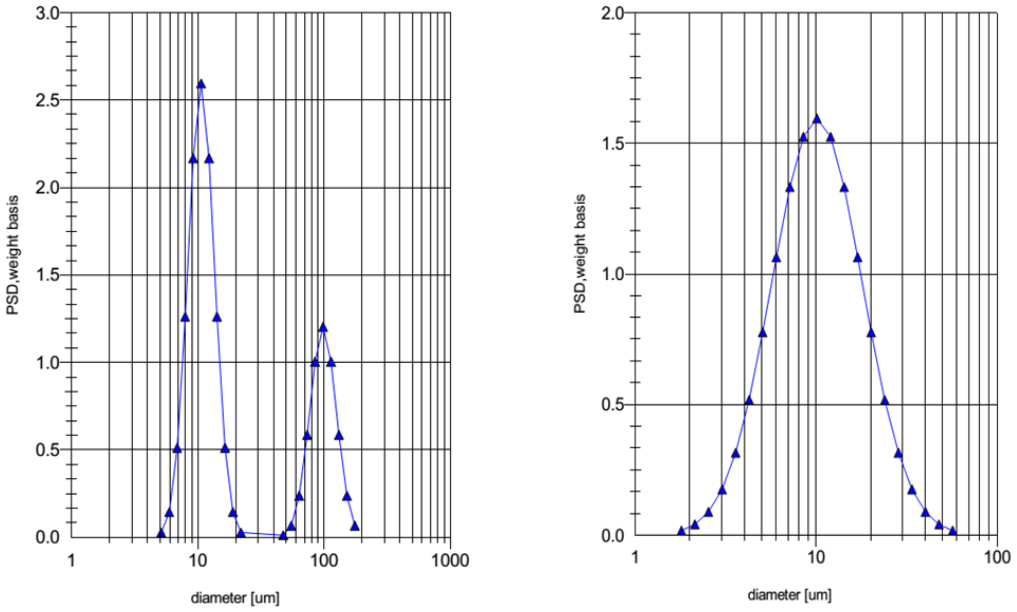

Fig. 5. Particle size distribution of KC and MKC.

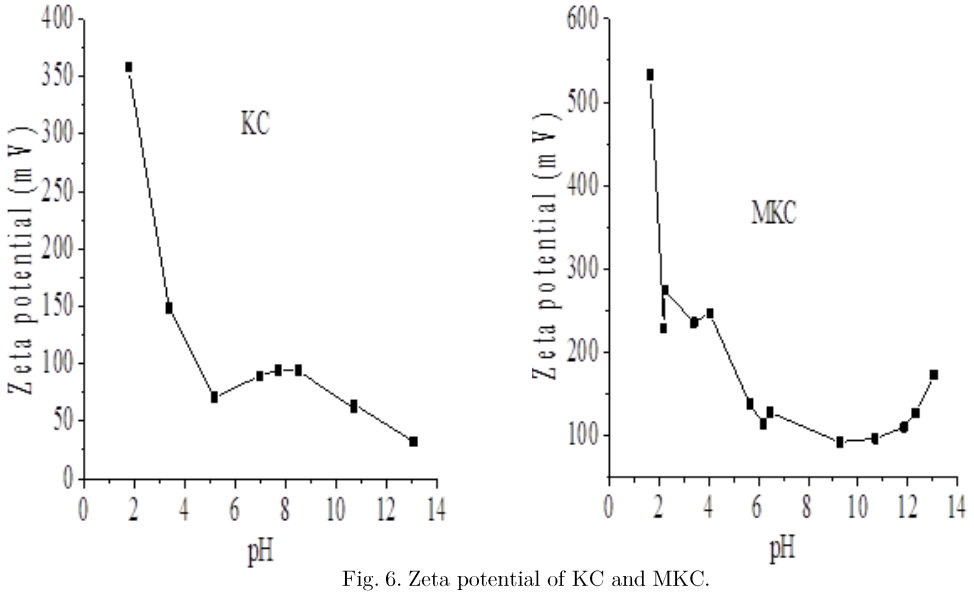

Fig. 6. Zeta potential of KC and MKC.

3.2 ADSORPTION

The effect of contact time on the amount of Cd^{2+} and Pb^{2+} ions adsorbed is presented in Fig. 7. The adsorption capacity was seen to increase with time. The amount of Cd^{2+} and Pb^{2+} ions adsorbed in mg/g by KC and MKC were calculated using equation:

$$q_e = \frac{(C_o - C_e)V}{M} \quad (1)$$

Where q_e is the amount adsorbed in mg/g, C_o and C_e are initial and final concentrations (mg/L) of adsorbates in solution; respectively while V and M are volumes (L) of Cd^{2+} and Pb^{2+} ions solution and weight (g) of KC and MKC used. The data obtained from the study were further evaluated for pseudo-first-order, pseudo-second-order, Elovich, intra-particle and liquid-film diffusion models. Pseudo-first-order model was given as:

$$-In(q_e - q_t) + Inq_e = k_1 t \quad (2)$$

On rearrangement Eq. 2 becomes

$$1 - \frac{q_t}{q_e} = \exp(-k_1 t) \quad (3)$$

The linearized form of the kinetic rate expression for a pseudo-second-order model is given as:

$$\frac{t}{q_t} = \frac{1}{K_2 q_e^2} + \frac{1}{q_e} t \quad (4)$$

where q_e is the amount of Pb^{2+} or Cd^{2+} adsorbed at equilibrium (mg/g), q_t is the amount of Pb^{2+} or Cd^{2+} (mg/g) adsorbed at time t (min) and k_1 (min^{-1}) and k_2 (g/mg/min) are the rate constants of the pseudo-first-order and pseudo-second-order models, respectively; for sorption of Pb^{2+} and Cd^{2+} ions. Plot of log (q_e-q_t) against time t, gave a linear relationship for pseudo-first-order model from which k_1 and equilibrium sorption capacity (q_e), were calculated from the slope and intercept respectively. For the pseudo-second-order, the parameters h_o which is the initial sorption rate and k_2 were determined from the slope and intercept of a plot of $\frac{t}{q_t}$ against t.

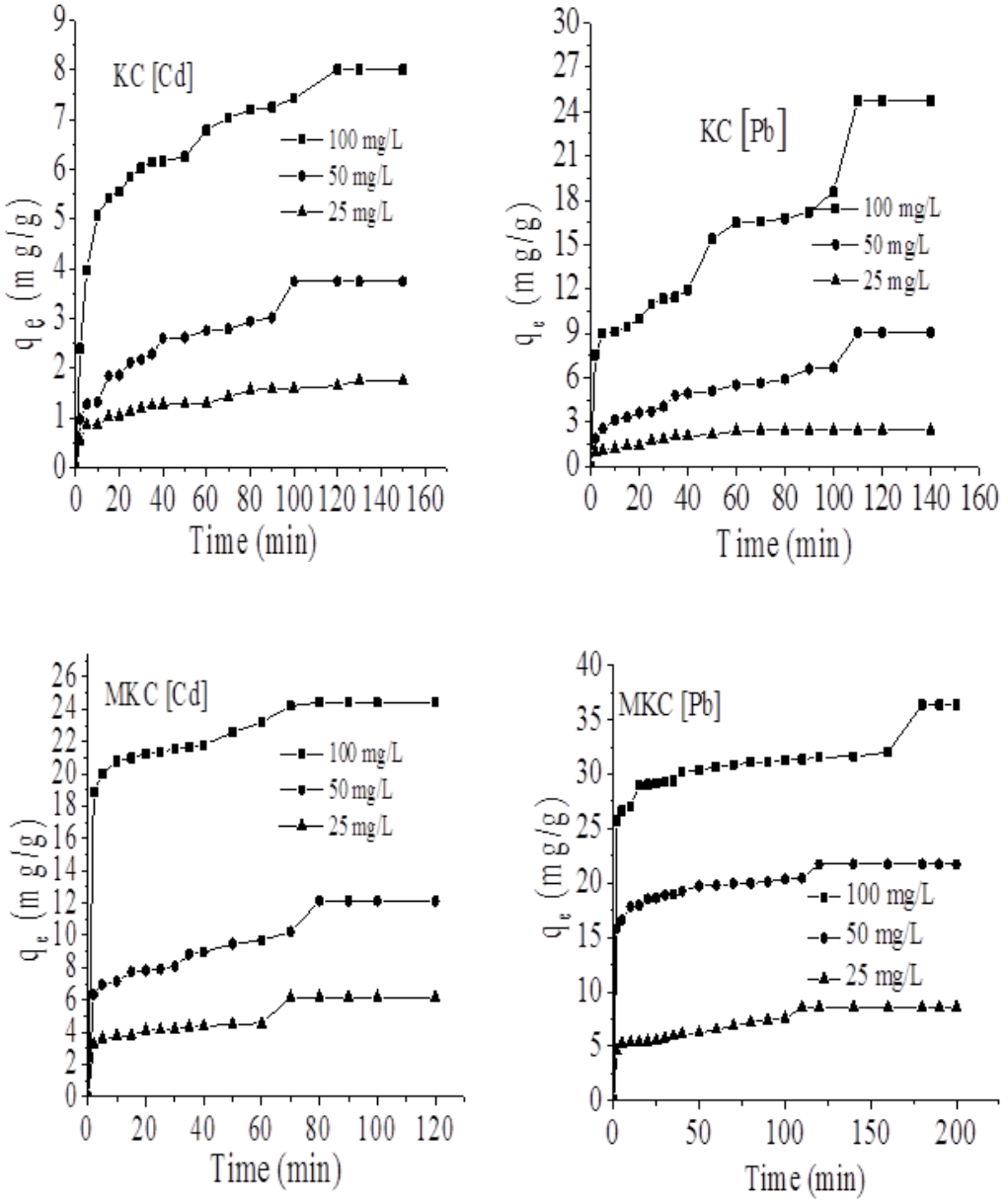

Fig. 7. Adsorption capacity of KC and MKC towards Cd and Pb at different concentration (25 – 100 mg/L) and time (298 K).

Table 1 compares the K_{ad}, h_o, qe and r^2 associated with pseudo-first-order and pseudo-second-order equations for sorption of Cd^{2+} ions on KC and MKC. K_{ad}, h_o and q_e increased with increase in concentration of Cd^{2+} ions. In both KC and MKC pseudo-second-order exhibited a better r^2 value indicating that the order of the adsorption of Cd^{2+} on KC and MKC follows a pseudo-second-order. Moreover, the qe, calculated values for pseudo-second-order agreed better with the experimental qe values which further supported the claim that the present adsorption process follows pseudo-second-order.

The adsorption capacity of KC and MKC was found higher for Pb^{2+} than Cd^{2+} which may be due to the higher ionic radius of Pb^{2+} (119 pm) than that of Cd^{2+} (95 pm). Since the ionic radius of Pb^{2+} is higher, the outermost electrons are more freely available for interaction with KC and MKC unlike in the case of Cd^{2+} where the inward pull from the nucleus on the outermost electrons is higher. The adsorption capacity for Cd^{2+} ions increased from 8.01 mg/g in KC to 24.41 mg/g in MKC. The present adsorption capacity by MKC towards Cd^{2+} is higher than values reported for *Trichoderma viride* biomass (Singh et al., 2010), modified corn stalk (Zheng, Dang, Yi, & Zhang, 2010), and *Lentinus edodes* (Zhang, Zeng, Ma, He, & Falandysz, 2012) but lower than value reported by Yuan et al (2016) for biogenic selenium nanoparticles (59.7 mg/g). The results for Pb^{2+} ions are presented in Table 2. The q_e and h_o increased with increase in concentrations. The r^2 values were also better for pseudo-second-order than pseudo-first-order.

Table 1. Comparison between K_{ad}, qe and r^2 associated with pseudo-first –order and pseudo-second-order equations for sorption of Cd^{2+} ions on KC and MKC.

Initial Cd^{2+} (mg/L)	Pseudo-first-order (KC)			Pseudo-second-order (KC)				
	K_1 (min^{-1})	q_e, cal (mg/g)	r^2	K_2 (g/mg/min)	q_e, cal (mg/g)	r^2	h_o (mg/g/min)	q_e, Exp (mg/g)
25	0.0083	1.08	0.968	0.0370	1.84	0.9851	0.1256	1.75
50	0.0064	2.53	0.9573	0.0104	4.19	0.9639	0.1815	4.00
100	0.0085	4.01	0.9521	0.0116	8.38	0.9935	0.8127	8.01

Initial Cd^{2+} (mg/L)	Pseudo-first-order (MKC)			Pseudo-second-order (MKC)				
	K_1 (min^{-1})	q_e, cal (mg/g)	r^2	K_2 (g/mg/min)	q_e, cal (mg/g)	r^2	h_o (mg/g/min)	q_e, Exp (mg/g)
25	0.0042	2.69	0.9266	0.0062	6.68	0.9580	0.5295	6.17
50	0.0066	5.85	0.9813	0.0063	13.02	0.9720	1.0717	12.14
100	0.0091	6.64	0.8000	0.0122	25.00	0.9980	7.6104	24.41

Table 2. Comparison between K_{ad}, qe and r^2 associated with pseudo-first –order and pseudo-second-order equations for sorption of Pb^{2+} ions on KC and MKC.

Initial Pb^{2+} (mg/L)	Pseudo-first-order (KC)			Pseudo-second-order (KC)				
	K_1 (min^{-1})	q_e, cal (mg/g)	r^2	K_2 (g/mg/min)	q_e, cal (mg/g)	r^2	h_o (mg/g/min)	q_e, Exp (mg/g)
25	0.0221	2.26	0.8644	0.0327	2.70	0.9918	0.2388	2.45
50	0.0046	6.76	0.9754	0.0082	7.29	0.9675	0.4371	7.00
100	0.0045	17.60	0.9579	0.0027	21.00	0.9426	1.1779	24.75

Initial Pb^{2+} (mg/L)	Pseudo-first-order (MKC)			Pseudo-second-order (MKC)				
	K_1 (min^{-1})	q_e, cal (mg/g)	r^2	K_2 (g/mg/min)	q_e, cal (mg/g)	r^2	h_o (mg/g/min	q_e, Exp (mg/g)
25	0.0056	4.03	0.9687	0.0075	9.17	0.9888	0.6265	8.58
50	0.0055	4.55	0.9273	0.0093	22.12	0.9984	4.5620	22.00
100	0.0021	6.90	0.8383	0.0039	35.59	0.9888	4.9358	36.41

The adsorption capacity also increased from 24.75 mg/g in KC to 36.41 mg/g in MKC. The value obtained for MKC towards Pb^{2+} is higher than values reported for Walnut (Bulut & Tez, 2007), CuO nanostructures (Farghali, Bahgat, Allah, & Khedr, 2013) and Sugar cane saw dust (Putra et al., 2014) but lower than that of *Cassia fistula* seed carbon (Senniappan, Palanisamy, Shanmugam, & Gobalsamy, 2017). This observed increase in the adsorption capacity after functionalization may be attributed to the presence of the amide function group. This suggests that the amide group may have participated in the adsorption process via cation exchange mechanism as proposed in Scheme 3. It was observed that the BET surface area reduced after surface functionalization whereas the adsorption capacity towards Cd^{2+} and Pb^{2+} increased. This observation revealed that the surface functionalization of KC played an important role in the adsorption process. However, the surface functionalization was effective enough to cover up for the reduction in BET surface area which is about 18.75% (from 16 m^2/g to 13 m^2/g).

Moreover, the reduction in surface area may not have seriously affected or reduced the amounts of specific active sites on KC which were involved in the adsorption process.

The data were further subjected to the Elovich model equation has expressed below:

$$\frac{dq_t}{d_t} = \alpha\, esp(-\beta q_t) \quad (5)$$

where α is the initial adsorption rate (mg/g min) and β is the adsorption constant (g/mg). A plot of q_t versus ln t gave a linear trace with a slope of (1/β) and an intercept of 1/β ln(αβ). The values of α and β are presented in Table 3.

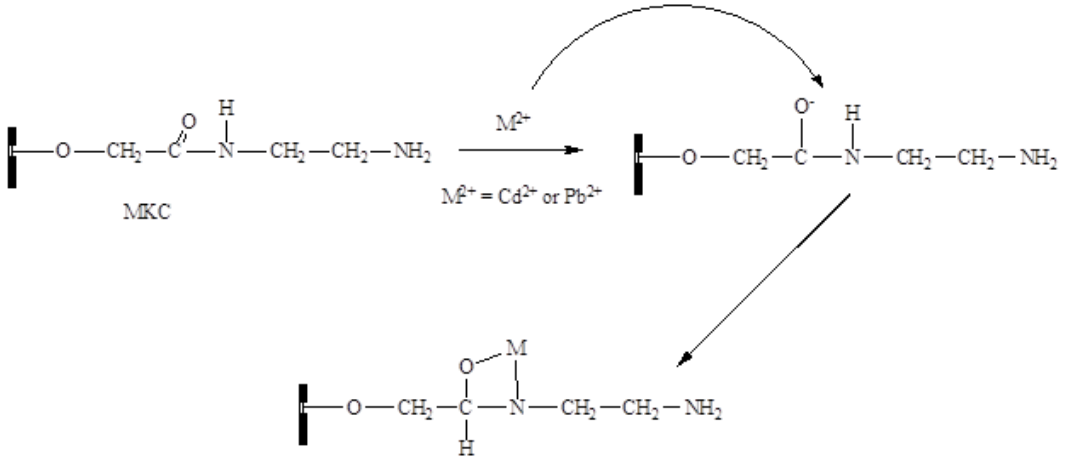

Scheme 3. Proposed adsorption mechanism of Cd^{2+} and Pb^{2+} on MKC.

Table 3. Kinetic model parameters for the sorption of Pb^{2+} and Cd^{2+} on KC and MKC.

Model	Parameter	KC (Cd)	MKC (Cd)	KC (Pb)	MKC (Pb)
Liquid film diffusion	K_{id} (g/mg/min)	0.0040	0.0029	0.0088	0.0017
	r^2	0.9411	0.9095	0.9276	0.8000
Elovich	β (g/mg)	0.8171	0.3427	0.6930	0.6744
	α (mg/g/min)	6.4115	21.6890	32.2813	41.4188
	r^2	0.9823	0.8031	0.9161	0.9734
Intra-particle diffusion	K_{id} (mg/g/$min^{1/2}$)	0.4465	1.3350	0.6173	0.5142
	r^2	0.9036	0.9406	0.9589	0.9000

The diffusion distribution of Cd^{2+} and Pb^{2+} ions on KC and MKC was evaluated using intraparticle diffusion model; this was considered in term of the total surface area of KC and MKC which may be taken to be made up of both external and internal surfaces. The intraparticle diffusion model was estimated as described by Srivastava et al (Srivastava, Swamy, Mall, Prasad, & Mishra, 2006):

$$q_t = K_{id}T^{0.5} + C \quad (6)$$

From equation 6, k_{id} is the intraparticle diffusion rate constant (mg/g/min$^{0.5}$) and C (mg/g) is a constant that describes the thickness of the boundary layer. On plotting q_t versus $T^{0.5}$, a linear plot was obtained indicating that sorption process was controlled by intra-particle diffusion. The respective K_{id} and r^2 values are shown in Table 3. Liquid film diffusion model was also used to study the movement of Cd^{2+} and Pb^{2+} ions from the liquid phase up to the solid phase boundary during the adsorption process.

$$In\,(1-F) = -K_{id}t \quad (7)$$

Where F is defined as:

$$F = \frac{q_e}{q_t} \quad (8)$$

K_{id} is the adsorption rate constant and t is time. A linear plot of –In (1-F) versus t was obtained which suggests that the kinetics of the sorption process may also be influenced by diffusion through the liquid surrounding KC and MKC (Ekpete, Horsfall & Spiff, 2012a). The effect of adsorbent weight on the sorption of Cd^{2+} and Pb^{2+} ions are presented in Fig. 8; it was noticed that the adsorption capacity of KC and MKC decreased as their weight increases.

Fig. 9 shows the effect of pH on adsorption process. It was observed that the capacity of KC and MKC to remove Cd^{2+} and Pb^{2+} ions from solution increased with increase in pH.

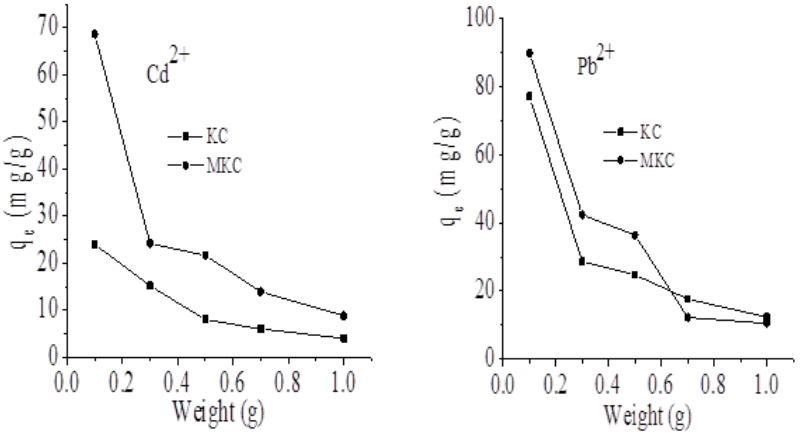

Fig. 8. Effect of weight of KC and MKC on adsorption of Cd^{2+} and Pb^{2+} from aqueous solution (100 mg/g) at 298K.

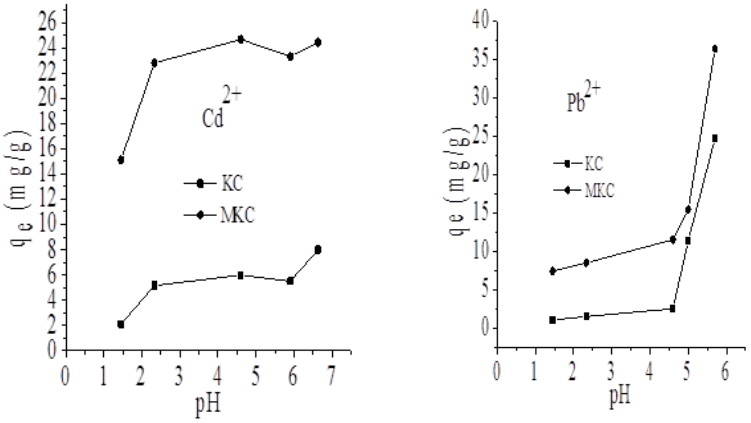

Fig. 9. Effect of solution (100 mg/L) pH on the sorption of Cd^{2+} and Pb^{2+} ions by KC and MKC at 298 K.

3.3 ADSORPTION ISOTHERM

It is paramount to establish the most suitable correlation for the equilibrium adsorption curve for the sorption of Cd^{2+} and Pb^{2+} ions on KC and MKC. To this effect, data obtained were subjected to some isotherm equations, namely; Langmuir, Freundlich and Temkin. Of the three equations, Freundlich and Temkin fitted well for the isotherm plots. The Freundlich isotherm is characteristic of heterogeneous surface, this is expressed as:

$$q_e = K_f C_e^{\frac{1}{n}} \quad (9)$$

The linearized form is given as:

$$log\, q_e = logK_f + \frac{1}{n}\, logC_e \quad (10)$$

K_f (mg/g) is the Freundlich isotherm constant which indicates adsorption capacity, C_e (mg/L) is the equilibrium concentration of Cd^{2+} and Pb^{2+}, q_e (mg/g) is the amount of Cd^{2+} and Pb^{2+} adsorbed at equilibrium and n is the adsorption intensity. Parameters K_f and n play important role in understanding the adsorption process. When n = 1, then the partition between the liquid and solid phases are independent of the concentration; If 1/n = <1, it indicates a normal adsorption but when 1/n = >1, it indicates cooperative adsorption (Goldberg, Tabatabai, Sparks, Al-Amoodi, & Dick, 2005). The results obtained for the Freundlich parameters are presented in Table 4 indicating the values of 1/n for Cd^{2+} and Pb^{2+} ions to be 1 suggesting a linear adsorption isotherm.

The Temkin isotherm contains a parameter that explicitly takes the adsorbate-adsorbent interaction into consideration. This is expressed as:

$$q_e = \left(\frac{RT}{b}\right) In(AC_e) \quad (11)$$

$$q_e = BInA + BInC_e \quad (12)$$

Note that:

$$B = \frac{RT}{b} \quad (13)$$

From equations 12 and 13, B (J/mol) is the constant related to heat of adsorption, A (L/g) is the Temkin isotherm equilibrium binding constant, b is the Temkin isotherm constant, R is the gas constant (8.314 J/mol/K) and T is the absolute temperature (K). The parameters were determined from the slope and intercept of a linear plot of q_e against ln C_e. The values of B, A and b are shown in Table 4. MKC had higher heat of adsorption than KC which is higher for Pb^{2+} than Cd^{2+} ions.

3.4 SORPTION THERMODYNAMICS

Experimental data obtained from the effect of temperature on the sorption of Cd^{2+} and Pb^{2+} ions on KC and MKC were analyzed to determine some thermodynamic parameters such as Gibb's free energy change (ΔG^o), enthalpy change (ΔH^o) and entropy change (ΔS^o). The adsorption equilibrium constant b_o was estimated from the expression (Ekpete, Horsfall, & Spiff, 2012b):

$$b_o = \frac{C_e}{C_o} \quad (14)$$

$$\Delta G^o = -RTInb_o \quad (15)$$

$$\Delta G^o = \Delta H^o - T\Delta S^o \quad (16)$$

Table 4. Freundlich and Temkin isotherm constants for the sorption of Pb^{2+} and Cd^{2+} ions by KC and MKC.

Freundlich model				
	KC (Cd)	MKC (Cd)	KC (Pb)	MKC (Pb)
K_f (mg/g)	1.9997	2.0002	2.0000	1.9981
n	1.0000	0.9999	0.9999	1.0002
r^2	0.9998	1.0000	0.9998	1.0000

Temkin				
	KC (Cd)	MKC (Cd)	KC (Pb)	MKC (Pb)
A	5.8892	61.3400	69.225	98.314
B	4.8731	22.041	29.759	31.361
b	508.4181	112.4074	83.2545	79.0017
r^2	0.9598	0.9984	0.9732	0.9960

where C_o and C_e are the initial and equilibrium concentrations of Cd^{2+} and Pb^{2+} ions, R is universal gas constant (8.314 J mol^{-1} K^{-1}) and T is the absolute temperature in K. The values of ΔH^o and ΔS^o were calculated from the slope and intercept of the linear plot of ln b_o against reciprocal of temperature (1/T). The values obtained for ΔG^o was positive nature which shows that energy is required to promote the adsorption of these metal ions on KC and MKC. The values of ΔG^o for KC and MKC are presented in Table 5 and Table 6 respectively. In the case of KC the value of ΔG^o increased with increase in temperature for Cd^{2+} ions while for Pb^{2+} ions, the value obtained decrease with increase in temperature. Values of ΔH^o and ΔS^o for KC and MKC are shown in Table 7. ΔS^o is negative for the sorption of Cd^{2+} ion on KC (-0.0055 KJ $mol^{-1}K^{-1}$) and MKC (-0.0001 KJ $mol^{-1}K^{-1}$) whereas in the case of Pb^{2+} ion, the value was positive for KC (0.0016 KJ $mol^{-1}K^{-1}$) and MKC (0.0081 KJ $mol^{-1}K^{-1}$).

ΔH^o was found positive for Cd^{2+} ion suggesting an endothermic process while the process was negative in the case of Pb^{2+} ion suggesting exothermic process.

Table 5. ΔG and q_e obtained at various temperatures for KC.

Cd				
T (K)	298	313	323	333
qe (mg/g)	8.008	12.845	16.180	19.618
ΔG (kJ $mol^{-1}K^{-1}$)	0.4323	0.7726	1.0497	1.3793
Pb				
T (K)	298	313	323	333
qe (mg/g)	24.746	17.115	11.013	7.160
ΔG (kJ $mol^{-1}K^{-1}$)	1.6922	1.0904	0.6679	0.4280

Table 6. ΔG and q_e obtained at various temperatures for MKC.

Cd				
T (K)	298	313	323	333
qe (mg/g)	23.569	18.138	15.745	11.146
ΔG (kJ $mol^{-1}K^{-1}$)	1.6595	1.1723	1.0156	0.6982
Pb				
T (K)	298	313	323	333
qe (mg/g)	36.410	6.250	5.370	4.980
ΔG (kJ $mol^{-1}K^{-1}$)	3.2265	0.3474	0.3051	0.2904

Table 7. Thermodynamic parameters obtained from plot of ln b_o vs 1/Tfor KC and MKC.

	KC		**MKC**	
Parameters	Cd	Pb	Cd	Pb
ΔH (kJ mol^{-1})	0.1058	-0.1850	-0.1390	-0.4545
ΔS (KJ $mol^{-1}K^{-1}$)	-0.0055	0.0016	-0.0001	0.0081

4. CONCLUSION

The present study evaluated the surface modification of kaolinite clay as a low-cost adsorbent for the removal of Pb^{2+} and Cd^{2+} ions from aqueous solution. Adsorption of these metals was found to be monolayer, second-order-kinetic and controlled by both intra-particle diffusion and liquid film diffusion. The adsorption capacity of the kaolinite clay towards Pb^{2+} and Cd^{2+} increased after modification with ethylenediamine. This presents MKC as a suitable adsorbent for the removal of Pb^{2+} and Cd^{2+} from aqueous solution of waste water.

ACKNOWLEDGEMENTS

This research was supported by International Foundation for Science (IFS) water research grant (No W/5401-1). The authors are grateful to Department of Chemistry, Federal University of Minas Gerais for provision of equipment. Authors also acknowledge the support of Organization for the Prohibition of Chemical Weapons (OPCW).

CONFLICT OF INTEREST

The authors have no conflicts of interest to declare.

REFERENCES

Adewuyi, A., & Pereira, F. V. (2016). Nitrilotriacetic acid functionalized Adansonia digitata biosorbent: Preparation, characterization and sorption of Pb (II) and Cu (II) pollutants from aqueous solution. *Journal of advanced research*, *7*(6), 947-959.

Adewuyi, A., & Pereira, F. V. (2017). Chemical Modification of Cellulose Isolated from Underutilized Hibiscus sabdariffa via Surface Grafting: A Potential Bio-based Resource for Industrial Application. *Kemija u Industriji*, *66*.

Basra, S., Iqbal, Z., Ur-Rehman, H., & Ejaz, M. F. (2014). Time Course Changes in pH, Electrical Conductivity and Heavy Metals (Pb, Cr) of Wastewater Using Moringa oleifera Lam. Seed and Alum, a Comparative Evaluation. *Journal of applied research and technology*, *12*(3), 560-567.

Bhattacharyya, K. G., & Gupta, S. S. (2006). Pb (II) uptake by kaolinite and montmorillonite in aqueous medium: influence of acid activation of the clays. *Colloids and Surfaces A: Physicochemical and Engineering Aspects*, *277*(1-3), 191-200.

Bhattacharyya, K. G., & Gupta, S. S. (2008). Kaolinite and montmorillonite as adsorbents for Fe (III), Co (II) and Ni (II) in aqueous medium. *Applied Clay Science*, *41*(1-2),1-9.

Borisover, M., Gerstl, Z., Burshtein, F., Yariv, S., & Mingelgrin, U. (2008). Organic sorbate– organoclay interactions in aqueous and hydrophobic environments: sorbate– water competition. *Environmental science & technology*, *42*(19), 7201-7206.

Bulut, Y., & Tez, Z. (2007). Removal of heavy metals from aqueous solution by sawdust adsorption. *Journal of Environmental Sciences (China)*, *19*(2), 160-166.

Ekpete, O. A., Horsfall, M., & Spiff, A. I. (2012a). Kinetics of chlorophenol adsorption onto commercial and fluted pumpkin activated carbon in aqueous systems. *Asian J Nat Appl Sci*, *1*, 106-117.

Ekpete, O. A., Horsfall, M., & Spiff, A. I. (2012b). Removal of chlorophenol from aqueous solution using fluted pumpkin and commercial activated carbon. *As. J. Nat & App. Sci*, *1*(1), 2186-8476.

Fan, Q., Li, Z., Zhao, H., Jia, Z., Xu, J., & Wu, W. (2009). Adsorption of Pb (II) on palygorskite from aqueous solution: effects of pH, ionic strength and temperature. *Applied Clay Science*, *45*(3), 111-116.

Farghali, A. A., Bahgat, M., Allah, A. E., & Khedr, M. H. (2013). Adsorption of Pb (II) ions from aqueous solutions using copper oxide nanostructures. *Beni-Suef University Journal of Basic and Applied Sciences*, *2*(2), 61-71.

Farmered, V. (1974). The infrared spectra of minerals, mineralogical society. *Adlard & Son, Surrey, UK*.

Frost, R. L., Van Der Gaast, S. J., Zbik, M., Kloprogge, J. T., & Paroz, G. N. (2002). Birdwood kaolinite: a highly ordered kaolinite that is difficult to intercalate—an XRD, SEM and Raman spectroscopic study. *Applied Clay Science*, *20*(4-5), 177-187.

Galadima, A., & Garba, Z. N. (2012). Heavy metals pollution in Nigeria: causes and consequences. *Elixir pollution*, *45* (2012), 7917-7922.

Galadima, A., Garba, Z. N., Leke, L., Almustapha, M. N., & Adam, I. K. (2011). Domestic water pollution among local communities in Nigeria-causes and consequences. *European Journal of Scientific Research*, *52*(4), 592-603.

Goldberg, S., Tabatabai, M., Sparks, D. L., Al-Amoodi, L., & Dick, W. (2005). Equations and models describing adsorption processes in soils. *Soil Science Society of America Book Series*, *8*, 489.

Guerra, D. L., Airoldi, C., & de Sousa, K. S. (2008). Adsorption and thermodynamic studies of Cu (II) and Zn (II) on organofunctionalized-kaolinite. *Applied Surface Science*, *254*(16), 5157-5163.

Gupta, S. S., & Bhattacharyya, K. G. (2008). Immobilization of Pb (II), Cd (II) and Ni (II) ions on kaolinite and montmorillonite surfaces from aqueous medium. *Journal of environmental management*, *87*(1), 46-58.

Hanaor, D., Michelazzi, M., Leonelli, C., & Sorrell, C. C. (2012). The effects of carboxylic acids on the aqueous dispersion and electrophoretic deposition of ZrO2. *Journal of the European Ceramic Society*, *32*(1), 235-244.

Koh, S. M., & Dixon, J. B. (2001). Preparation and application of organo-minerals as sorbents of phenol, benzene and toluene. *Applied Clay Science*, *18*(3-4), 111-122.

Laouchedi, D., Bezzazi, B., & Aribi, C. (2017). Elaboration and characterization of composite material based on epoxy resin and clay fillers. *Journal of applied research and technology*, *15*(2), 190-204.

McMillan, P. F., Wolf, G. H., & Poe, B. T. (1992). Vibrational spectroscopy of silicate liquids and glasses. *Chemical Geology*, *96*(3-4), 351-366.

Manohar, D. M., Noeline, B. F., & Anirudhan, T. S. (2006). Adsorption performance of Al-pillared bentonite clay for the removal of cobalt (II) from aqueous phase. *Applied Clay Science*, *31*(3-4), 194-206.

Mirbolooki, H., Amirnezhad, R., & Pendashteh, A. R. (2017). Treatment of high saline textile wastewater by activated sludge microorganisms. *Journal of Applied Research and Technology*, *15*(2), 167-172.

Moore, D. M., & Reynolds, R. C. (1989). *X-ray Diffraction and the Identification and Analysis of Clay Minerals* (Vol. 322, p. 321). Oxford: Oxford university press.

Nishikiori, H., Shindoh, J., Takahashi, N., Takagi, T., Tanaka, N., & Fujii, T. (2009). Adsorption of benzene derivatives on allophane. *Applied Clay Science*, *43*(2), 160-163.

Pouya, E. S., Abolghasemi, H., Fatoorehchi, H., Rasem, B., & Hashemi, S. J. (2016). Effect of dispersed hydrophilic silicon dioxide nanoparticles on batch adsorption of benzoic acid from aqueous solution using modified natural vermiculite: An equilibrium study. *Journal of applied research and technology*, *14*(5), 325-337.

Putra, W. P., Kamari, A., Yusoff, S. N. M., Ishak, C. F., Mohamed, A., Hashim, N., & Isa, I. M. (2014). Biosorption of Cu (II), Pb (II) and Zn (II) ions from aqueous solutions using selected waste materials: Adsorption and characterisation studies. *Journal of Encapsulation and Adsorption Sciences*, *4*(01), 25.

Saikia, B. J., & Parthasarathy, G. (2010). Fourier transform infrared spectroscopic characterization of kaolinite from Assam and Meghalaya, Northeastern India. *Journal of Modern Physics*, *1*(04), 206.

Senniappan, S., Palanisamy, S., Shanmugam, S., & Gobalsamy, S. (2017). Adsorption of Pb (II) from aqueous solution by Cassia fistula seed carbon: kinetics, equilibrium, and desorption studies. *Environmental Progress & Sustainable Energy*, *36*(1), 138-146.

Sidheswaran, P., Bhat, A. N., & Ganguli, P. (1990). Intercalation of salts of fatty acids into kaolinite. *Clays Clay Miner*, *38*(1), 29-32.

Singh, R., Chadetrik, R., Kumar, R., Bishnoi, K., Bhatia, D., Kumar, A., ... & Singh, N. (2010). Biosorption optimization of lead (II), cadmium (II) and copper (II) using response surface methodology and applicability in isotherms and thermodynamics modeling. *Journal of Hazardous Materials*, *174*(1-3), 623-634.

Srivastava, V. C., Swamy, M. M., Mall, I. D., Prasad, B., & Mishra, I. M. (2006). Adsorptive removal of phenol by bagasse fly ash and activated carbon: equilibrium, kinetics and thermodynamics. *Colloids and surfaces a: physicochemical and engineering aspects*, *272* (1-2), 89-104.

Unuabonah, E. I., & Taubert, A. (2014). Clay–polymer nanocomposites (CPNs): Adsorbents of the future for water treatment. *Applied clay science*, *99*, 83-92.

Yuan, F., Song, C., Sun, X., Tan, L., Wang, Y., & Wang, S. (2016). Adsorption of Cd (II) from aqueous solution by biogenic selenium nanoparticles. *RSC Advances*, *6*(18), 15201-15209.

Zhang, D., Zeng, X., Ma, P., He, H., & Falandysz, J. (2012). The sorption of Cd (II) from aqueous solutions by fixed Lentinus edodes mushroom flesh particles. *Desalination and Water Treatment*, *46*(1-3), 21-31.

Zheng, L., Dang, Z., Yi, X., & Zhang, H. (2010). Equilibrium and kinetic studies of adsorption of Cd (II) from aqueous solution using modified corn stalk. *Journal of hazardous materials*, *176*(1-3), 650-656.